IRAQI Academic Scientific Journals

Tikrit Journal of Engineering Sciences (2021) 28 (2): 1-14.

ISSN: 1813-162X (Print) ; 2312-7589 (Online)

Tikrit Journal of Engineering Sciences

available online at: http://www.tj-es.com

TJES Tikrit Journal of Engineering Sciences

College of Engineering

Noor Hashim Hamed. Object-Based Method for Urban Extraction through Using Quick Bird Satellite Imagery, LiDAR Data and Digital Urban Geomatics Techniques . *Tikrit Journal of Engineering Sciences* 2021; **28**(2): 1- 14.

Noor Hashim Hamed*

Department of Civil Engineering /
University of Technology/ Baghdad / Iraq

***Keywords*:**

LiDAR, ANN, RF, SVM, urban extraction, eCognition software, ArcGIS.

A R T I C L E I N F O

Article history:

Received 16 Aug. 2020
Accepted 09 Sep. 2020
Available online 25 June 2021

Object-Based Method for Urban Extraction through Using Quick Bird Satellite Imagery, LiDAR Data and Digital Urban Geomatics Techniques

A B S T R A C T

Urban extraction mapping has become increasingly important in recent years and particularity extraction urban features based on remotely sensed data such as high-resolution imagery and LiDAR data. Though the researchers used the high spatial resolution image to extract urban area but he methods are still complex and still there are challenges associated with combining data that were acquired over differing time periods using inconsistent standards. So, this study will focus on the extraction of urban area based on an object-based classification method with integration of Quickbird satellite image and digital surface elevation (DSM) extracted from LiDAR data for the Rusafa city of Baghdad, Iraq. All the processes were done in eCognition and ArcGIS software for feature extraction and mapping, respectively. The overall methodological steps proposed in this research for the extraction of urban area using object-based method. In addition of that both the image data and LiDAR-derived DSM were integrated based on the eCognition software for extraction urban map of Rusafa city, Baghdad. Finally, the results indicated that the Artificial Neural Networks (ANN) model achieved the highest training and testing accuracies and performed the best compared to RF and Support Vector Machines (SVM) methods. And also, the results showed that the Artificial Neural Networks (ANN) had capability to extract the boundaries of the buildings and other urban features more accurately than the other two methods. This could be interpreted as the Artificial Neural Networks (ANN) model can learn complex features by the optimization process of the model and its multi-level feature extraction property.

DOI: http://doi.org/10.25130/tjes.28.2.01

* *Corresponding author: E-mail:* 40166@uotechnology.edu.iq.

طريقة كائنية الاعتماد للاستخلاص الحضري باستخدام صور للقمر الصناعي كوك بيرد وبيانات ليدار وتقنيات الجيوماتيك الحضرية الرقمية

نور هاشم حميد قسم الهندسة المدنية/ الجامعة التكنولوجية

الخلاصه

أصبح رسم الخرائط الحضرية لاستخراج المعالم الحضرية بناءً على البيانات المستشعرة عن بُعد مثل الصور عالية الدقة وبيانات LiDAR مهمًا بشكل متزايد في السنوات الأخيرة. على الرغم من أن الباحثين استخدموا الصورة ذات الدقة المكانية العالية لاستخراج المنطقة الحضرية ، إلا أنها لا تزال معقدة في الأساليب والتحديات المرتبطة بدمج البيانات التي تم الحصول عليها على مدى فترات زمنية مختلفة باستخدام معايير غير منسقة. لذلك ، ستركز هذه الدراسة على استخراج المناطق الحضرية بالاعتماد على الخصائص الطيفية و المكانية للمعالم و تجزئتها مع خلال دمج صورة الأقمار الصناعية Quickbird مع الارتفاع الرقمي للسطح (DSM) المستخرجة من بيانات LiDAR لمدينة الرصافة بغداد ، العراق. تم إجراء جميع العمليات في برنامج eCognition و ArcGIS لاستخراج المعالم ورسم الخرائط ، على التوالي بخطوات منهجية شاملة ومقترحة في هذا البحث لاستخراج المناطق الحضرية باستخدام أسلوب قائم على الكائنات. بالإضافة إلى ذلك ، تم استخدام كل من بيانات الصورة و DSM المشتق من LiDAR على أساس برنامج eCognition لاستخراج الخريطة الحضرية لمدينة الرصافة ، بغداد. أخيرًا، أشارت النتائج إلى أن نموذج ANN حقق أعلى درجات دقة التدريب والاختبار وأداء أفضل مقارنة بطريقتين RF و SVM. وأظهرت النتائج أيضًا أن شبكة ANN لديها القدرة على استخراج حدود المباني والميزات الحضرية الأخرى بدقة أكبر من الطريقتين الأخريين. يمكن تفسير ذلك لأن نموذج ANN يمكنه تعلم الميزات المعقدة من خلال عملية تحسين النموذج وخاصية استخراج الميزات متعددة المستويات.

1. INTRUDACTION

Urban mapping has become increasingly important in recent years [1-4], particularity extraction of urban features from remotely sensed data such as high-resolution imagery and LiDAR (Light Detection and Ranging) data [5-8]. Information about urban areas is widely used in GIS (Geographic Information System) applications including forestry, agriculture, geology and landscape studies. Urban information play important roles, for example, in mapping forest carbon in urban ecosystems [9], mapping individual trees in urban areas [10], in studies that use urban features (e.g., urban land use) for geological hazards [11], and in many landscape studies [12].

Urban feature extraction has been a challenging topic in remote sensing for years. This is mainly due to the limitations of the current sensors and the complexity of the urban environments. Urban areas often consist of different materials which have various material components such as minerals, vegetation, and other artificial features. Urban areas are characterized by a very high degree of spectral heterogeneity. Urban materials are also used for different purposes such as roof and road materials which add additional challenges to the urban feature extraction. Though these features are different, but they are similar in reflectance properties. Urban materials also get deteriorated with time which makes similar features look different spectrally and spatially. This problem induces a significant degree of spectral intra-class confusion. Finally, urban features may have complex geometry which requires specific spatial features that need to be calculated to enable significant separation of the features by the classifiers. Those lead to a substantial increase in heterogeneity in the measured spectral response of urban materials.

A number of previous works have investigated the use of remotely sensed data for urban mapping. Two types from urban extraction methods such as in general (pixel-based and object-based). Pixel-based methods use pixel information to extract urban features while object-based methods group image pixels into objects based on spectral and spatial information. Recent studies are more focused on object-based methods because they provide more accurate feature extraction and the outputs are GIS ready data which can be used for the targeted applications without much data conversion and post editing.

Studies such as by Benediktsson et al., [13] used 1C (IRS-1C) and IKONOS images to extract urban features with object-based methods. The classification was based on neural networks and its results suggested the selection of features which are a challenging task and needs further developments. Sensing HX-PE and R [14] proposed a model to extract urban built-up land features from Landsat thematic mapper and enhanced thematic mapper plus imagery. This study used spectral indices such as normalized difference built-up index (NDBI), modified normalized difference water index (MNDWI), and soil adjusted vegetation index (SAVI) to identify three major urban land-use classes such as built-up land, open water body, and vegetation. The results showed that the technique is effective and reliable through the overall accuracy ranging 91.5% - 98.5%. Myint et al., [15] used object-based classifier on QuickBird image to identify urban classes compared with the traditional classification algorithms. This study demonstrated that the object-based classifier (90.40%) is a significantly better approach than the classical per-pixel classifiers (maximum likelihood) (67.60%). Ahmed et al., [16] proposed an object level model based on a decision tree algorithm on SPOT image. The overall accuracy

of the proposed model was 96% and the Kappa index was 0.95. In addition, Ahmed et al., [17] proposed an object-based model through integration of Quickbird and Sentinel-1 data for several types of vegetation mapping. The method consists of four primary steps that image segmentation, Taguchi optimization, attributes selection using random forest, and rule-based feature extraction. The model achieved an overall accuracy of 0.87 for urban tree class. More recently, Chen et al., [18] combined deep learning with object-based image analysis for the extraction of urban water bodies from high-resolution imagery. The proposed model consists of three major steps which were segmentation based on an adaptive simple linear iterative clustering algorithm, designed a new convolutional neural network (CNN) through training this model on two classes: one including water or with no-water pixel. Experimental results showed that the proposed method achieved higher accuracy (99.14%). Other scholars have investigated integrated data for urban mapping in attempts to improve the accuracy of the models. Priem and Canters [19] integrated a high-resolution APEX hyper spectral image and a discrete waveform LiDAR dataset for urban mapping. Their results suggested that the proposed models could contribute to improve classification accuracies. Zhang et al., [20] tested the performance of a parcel-based land use classification method using random forest and LiDAR data. They suggested that the proposed technique is appropriate for the detailed urban feature extraction including mixed residential and commercial building. Sameen and Pradhan [21] developed a method based on object-based image classification with novel two-stage segmentation for the urban road extraction from high spatial resolution images and LiDAR data. To realize accurate feature extraction, they optimized the process for segmentation and classification which are main tasks of a classification problem within the object-based framework. Their approach could obtain reliable urban road extraction and the proposed optimization method could help improving the accuracy of the outputs. Li et al., [22] proposed an object-based classification method for the urban mapping from airborne LiDAR and multi-spectral image data. Their approach showed promise for large-area classification especially in forested areas. A recent work by Rizeei and Pradhan [5] combined high-resolution imagery and LiDAR data for the generation of urban maps. They explored the effects of image orthorectification on the accuracy of the maps. They showed that orthorectification is an important step in urban mapping and may significantly impact the final outputs. Degerickx et al., [23] developed Multiple Endmember Spectral Mixture Analysis (MESMA) for the extraction of urban features from multispectral and LiDAR data. They also used feature selection to improve the results. Their approach could be used for mapping of structurally diverse ecosystems, such as urban environments.

This study will focus on the extraction of urban area based on an object-based classification method with integration of Quickbird satellite images and digital surface elevation (DSM) extracted from LiDAR data for the Rusafa city of Baghdad, Iraq. All the processes were done in eCognition and ArcGIS software for feature extraction and mapping, respectively.

2. DATASETS

The study area of this research is a part of Al-Rusafa which is located in Baghdad at (44.45°, 44.46°) longitudes and (33.34°, 33.34°) latitude as shown in Fig.1. It is the most important administrative district in Baghdad among the nine administrative districts. The area with high population and different land uses such as (commercials, industrials, administrates, services, educations …etc).

For the validation of the proposed classification technique, two datasets over the study area were used including Quickbird satellite image and LiDAR. The Quickbird image was acquired on 2010 in a resolution of 60 cm. The image data for the study area are in three RGB bands. Instead, the LiDAR data are defined in a three-dimensional coordinate system (i.e. point clouds). This research used airborne LiDAR data of 0.5 m resolution captured on 2010 to obtain a very high-resolution DSM.

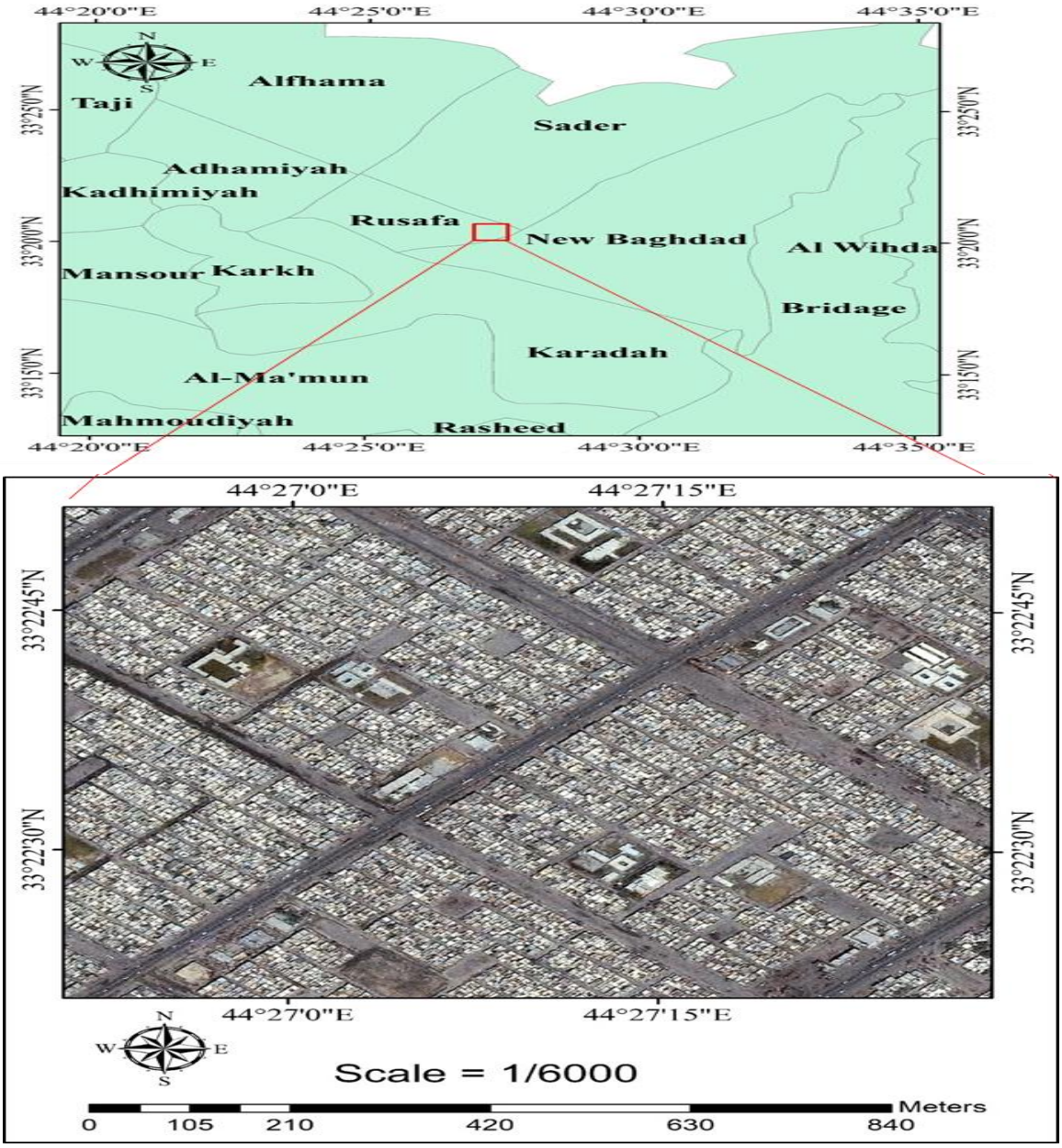

Fig. 1. Shows the Quickbird satellite image used in the current study

3. METHODOLOGY

The overall methodological steps proposed in this research for the extraction urban area using object-based method is presented in Fig. 2. The first is data pre-processing which included preparing the data and correcting them for spectral and spatial enhancement. The usual problem of the malfunction errors and sensor degradation lead to create these errors. A pre – process method for the Quickbird image will be done to correct the radiometric and geometric from the errors in the image. Then, the LiDAR data was corrected, and a DSM product was extracted. So, the first step is removing these errors before building the rule sets or generating the classification map which is considered an important step. After that, both the image data and LiDAR-derived DSM were integrated based on the eCognition software which offers a segmentation technique called multiresolution segmentation algorithm. Then, samples were collected from urban and non-urban areas. These samples were used to create a set of rules. The artificial neural network (ANN) classifier was thereafter applied on the mage objects to obtain the classification map of the study area. Also an Overall Accuracy and Kappa index will be sure to validate this method in this paper. Finally, a map with a special case as a thematic procedure of AL-Rusafa city was extracted and tested on samples not used during the training process.

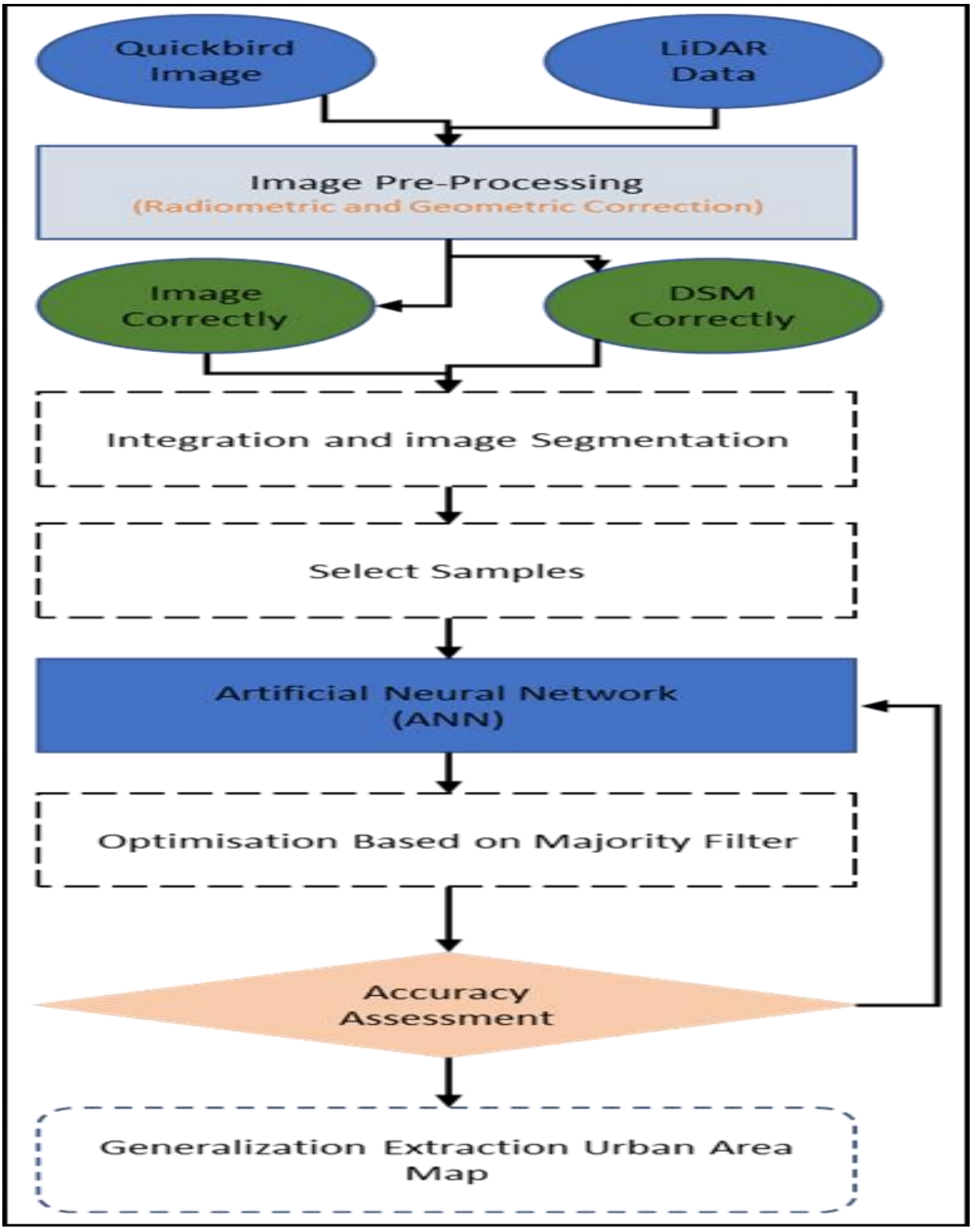

Fig. 2. Shows the overall methodology propose

3.1 *Digital Image Preprocessing (DIP)*

It is important to make sure that the remote sensing data is accurate and contains less noise before performing any image processing steps. In this paper, the Quickbird image was pre-processed in two

methods. The first method as in step was the digital numbers of the original image to be converted into reflectance.This method showing the effects of sun light, atmospheric layer, and improved the spectral information of the image to be reduced. In the second method, A geometric correction with set of projection coordinate were be done for the image .A final digital thematic map of the study area was done by the classification of the image with building Geo database as in GIS layers . The image which is processed of Quickbird image will used for the classification and segmentation.

On the other hand, DSM of LiDAR is built on the basis of cloud points with the extension of LAS. The multi-scale curves classification algorithm (MCC) was applied to classify the LiDAR returns to groundwater and offshore points. The algorithm integrates rotation filtering with a scale component and variable curvature tolerance. Using the thin plate spline method, a surface is set at different resolutions and the points are graded according to a progressive curvature parameter. If the resolution increases to compensate for the slope effect and normalizing the data, the order of rotation tolerance increases. Filtering windows (1x1) were used to filter DSMs extracted from the LiDAR data shown in Fig. 3.

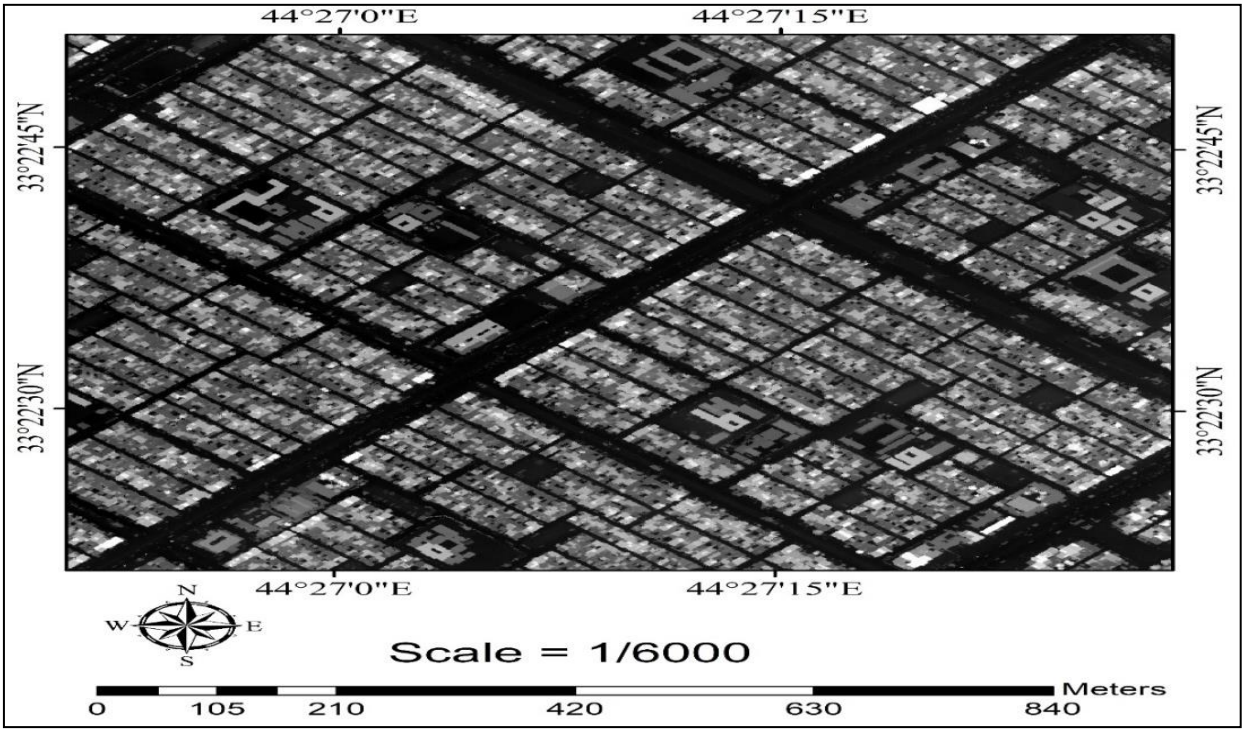

Fig.3. The LiDAR-derived DSM data

3.2 *Image Segmentation*

Once the data was prepared for analysis, the image was subdivided into a non-overlapping and uniform region using a multi-resolution segmentation algorithm. This process was implemented in eCognition software. In this algorithm, three parameters were required, scale, shape and compactness. These parameters were selected by trial and error method. After several trails, it was discovered that a scale of 25, a size of 0.5, and compactness was best for use with the study area and data set. Based on the user-defined parameter values of the Multi-Resolution Sequencing algorithm, the image was separated, and the next step, the image objects were created for the classification process.

3.3 *Classification Methods*

3.3.1 Support Vector Machines (SVM)

Support vector machines (SVMs) are a set of related supervised learning methods used for classification and regression. SVM is a statistical classification method and given m labeled training samples, $\{(\overrightarrow{x_i}, \overrightarrow{y_i} | \overrightarrow{x_i} \in R^n, y_i \in \{-1,1\}, i = 1 \dots m$, SVM can generate a separation hypersurface with maximum generalization ability. Mathematically, the decision function can be formulated as follows:

$$d(\overrightarrow{x}) = \sum_{i=1}^{m} \alpha_i y_i K(\overrightarrow{x_i}, \overrightarrow{x}) + b \quad (1)$$

where α_i and b are the parameters determined by SVM learning algorithm, and $K(\overrightarrow{x_i}\overrightarrow{x})$ is the kernel function, which implicitly maps the samples to a high dimension space. The samples $\overrightarrow{x_i}$ with nonzero parameters α_i are called support vectors.

3.3.2 *Random Forest (RF)*

Random forest (RF) is a machine learning based classification model that uses randomized decision trees. It is an ensemble model that can be used both for classification and regression problems. Thus, it has been used for a variety of tasks including land cover mapping. Its main advantage is the ability of predominant execution on high dimensional data. It also internally performs an implicit feature selection using a small subset of the training data. The feature selection process is guided by an indicator called "Gini importance".

3.3.3 *Artificial Neural Networks (ANN)*

The machine learning has several tasks such as classification, regression, clustering, dimensionality reduction and others. These tasks depend on the required output as in the machine learning procedure. In classification-machine learning has many algorithms for this topic such as ANN, SVM, Gaussian processes, Decision trees and another algorithm. In this research the classification and ANN task to produce classification map (thematic map was taken

ANN model has two equations which are considered very important to improve the accuracy for ANN model. First equation for minimizing the error function as illustrated in(Equation 2), second equation for correcting to weight parameters such as computed and added to the previous values (Equation 3).

$$E = \frac{1}{2}\sum_{i=1}^{L}\left(d_j - o_j^M\right)^2 \quad (2)$$

$$\begin{cases} \Delta w_{i,j} = -\mu \dfrac{\partial E}{\partial w_{i,j}} \\ \Delta w_{i,j}(t+1) = \Delta w_{i,j} + \alpha \Delta w_{i,j}(t) \end{cases} \quad (3)$$

where d_j represents the desired output, o_j^M represents the current response of the node in the output layer, and L is the number of nodes in the output layer.

where $w_{i,j}$ is weight parameter between node i, j, Δ is represent a learning rate, α is represent a momentum factor t.

3.4 Evaluation Methods

Error matrix analysis is used to determine the Kappa statistic (K) and Overall Accuracy (OA) in order to achieve the best classification accuracy. The computation of OA is achieved by dividing the total sum of the major diagonal by the total number of pixels available in the error analysis matrix. The Kappa analysis is a technique of discrete multivariate deployed in many accuracy assessments. Kappa analysis is a measure of accuracy yields or K statistic is calculated based on Equation 4:

$$K = \frac{N\sum_{i=1}^{r} x_{ii} - \sum_{i=1}^{r}(x_i + x_{+i})}{N^2 - \sum_{i=1}^{r}(x_i + x_{+i})} \quad (4)$$

Where the number of rows in the matrix is represented by the symbol r. The symbol x_{ii} stands for the number of observations in the row. While column$i$, x_{i+} and x_{+i} represent the marginal totals for both row i and column i and N denotes the total number of pixels.

On the other hand, F-measure is measure that combines precision and recall is the harmonic mean of precision and recall, the traditional F-measure or balanced F-score:

$$F = 2.\frac{precision.recall}{precision + recall} \quad (5)$$

$$Recall = \frac{tp}{tp + fn} \quad (6)$$

$$Precision = \frac{tp}{tp + fp} \quad (7)$$

$$Accuracy = \frac{tp + tn}{tp + tn + fp + fn} \quad (8)$$

TP represents True Positives which is the number of examples of predicted positive that are actually positive. FP refers to False Positives which is the number of examplesof predicted positive that are actually negative. TN is the True Negatives represents the number of negative predictions that are truly negative, and FN is the False Negatives indicates the number of negative predictions that are truly positive.

4. RESULTS AND DISCUSSION

4.1 *Results of image segmentation*

Image segmentation groups the image pixels into homogenous objects that let object spatial, textural and geometric properties to be calculated. The new features extracted at object-level could boost the accuracy of the classification. Fig. 4 shows the segmentation results applied in this research. The segmentation of the study area was generated using the parameters shown in table 1. The classification models including RF, ANN, and SVM were applied to the segmentation data to generate the classified map of the study area. The image objects along with their attributes were used for the classification.

The parameters of the segmentation have impacts on the generated image objects and thereby the classification results. The default parameters that come with the eCognition software were shown in table 1 yielded poor classification results. Thus, the parameters were fine-tuned by the trial and error method to find more appropriate values of the parameters that could help to improve the classification results. The scale parameter controls the size of the generated image objects. This parameter depends on the scale of the image and the geometry of the urban features in the area. The scale of 25 was found suitable in the study area because it makes the generated objects accurately represent the urban features. Other two parameters i.e. shape, and compactness control the geometry of the generated image objects as well as the smoothness of the objects. All the three parameters are highly important in the proposed method. The values selected in this research may not be suitable for other areas and thus may need further tuning as needed depending on the urban environment of the study area.

Table 1.
Default and selected values of the segmentation parameters

Parameter	Default Value	Selected Value (best for the study area)
Scale	10	25
Shape	0.1	0.5
Compactness	0.5	0.5

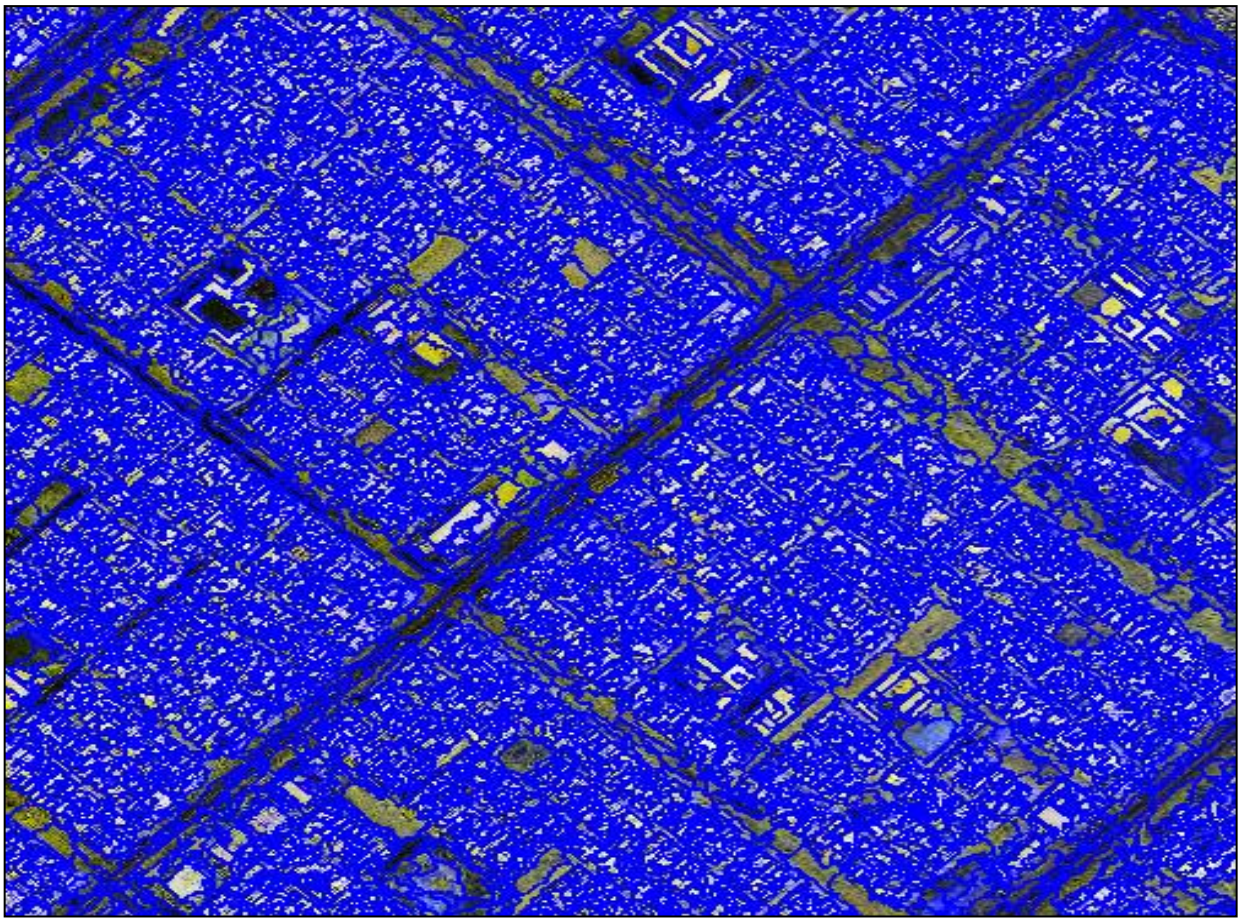

Fig . 4. Show the image objects created by using multi resolution segmentation algorithm.

4.2 Results of classification

The performance of the applied classification models using both the training and testing samples was shown in table 2. The results indicate that the ANN model performed the best compared to RF and SVM methods. The ANN model achieved the highest training and testing accuracies of overall accuracy (98.80%) and Kappa index (0.96) and overall accuracy (96.32%) and Kappa index (0.94) for the training and testing samples, respectively. RF outperformed the SVM method considering the training and testing samples. The overall accuracy and Kappa index of the model of RF were (91.44, 0.87) and (87.73, 0.84) for testing and training all the samples. The lowest accuracy was achieved by the SVM method. The SVM method achieved overall accuracy and Kappa index of (89.81%, 0.85) and (83.73%, 0.81) for the training and testing samples.

Table 2.
The training and testing accuracies obtained for the classification map of the study area with the proposed method.

Models	Training		Testing	
	Overall accuracy%	Kappa index	Overall accuracy%	Kappa index
SVM	89.81	0.85	83.73	0.81
RF	91.44	0.87	87.73	0.84
ANN	**98.80**	**0.96**	**96.32**	**0.94**

The ANN model because of its feature of extracting abstract information at multiple levels from the given image objects could help to achieve the best classification results. For the detailed assessment of the method, this research also calculated the accuracies of urban and non-urban classes separately based on Precision, Recall, and F-measure. The effects of these indicators are as follows. Precision indicated how many areas that the model determined to be positive were true positive areas. Recall indicated how many positive samples were judged to be positive by the model. F-measure was an index balancing precision against recall. The results are summarized in table 3. The model although achieved accuracies for non-urban areas higher than those of urban areas, it could produce an acceptable classification map for the study as shown in fig. 5. The average accuracies for both the urban and non-urban classes were Precision = 0.647, Recall = 0.652, and F-measure = 0.623.

Table 3
shows the detailed accuracy by class for the proposed models (ANN)

Class	True Positives Rate	False Positives Rate	Precision%	Recall%	F-Measure%
Urban	0.336	0.133	0.632	0.336	0.439
Non-Urban	0.867	0.664	**0.658**	**0.867**	**0.748**
Weighted Avg.	0.652	0.449	0.647	0.652	0.623

In addition, table 4 shows a contingency table which is also generally regarded as a confusion matrix. Confusion or error matrix is a specific table layout that is used to describe the performance of a classification model on a set of test data for which the true values are known. In this regard, there exist two classes. Hence, it can be represented by a 2 x 2 confusion matrix which can be arbitrarily large. The number of properly classified instances can be computed by summing the diagonals found in the matrix. This implies that other parameters in the matrix are wrongly classified (class "a" represents misclassified; "b" exactly twice; class "b" gets misclassified as "a" three times).

Table 4.
Shows the Confusion Matrix for the proposed models (ANN)

a	b	classified as
8850	17505	a = Urban
5143	33629	b = Non-urban

After the models have been tested, the classification maps with these models were generated for the study area. The classification map produced by the ANN model shown in Fig. 5 and by the RF and SVM are shown in Fig. 6 and Fig. 7. It is obvious from the results that the ANN had capability to extract the boundaries of the buildings and other urban features more accurately than the other two methods. This could be interpreted as the ANN model can learn complex features by the optimization process of the model and its multi-level feature extraction property. However, the ANN model may require additional computing time and optimization processes than the other two models. This could add computational challenges and thus it is suggested that it can only be applied in areas with complex urban features. It also helps to learn features from multi-modality datasets as is the case of this research Quickbird and LiDAR. For the applications with single dataset, other two methods may be good alternatives especially for rapid assessment of urban environments of an area.

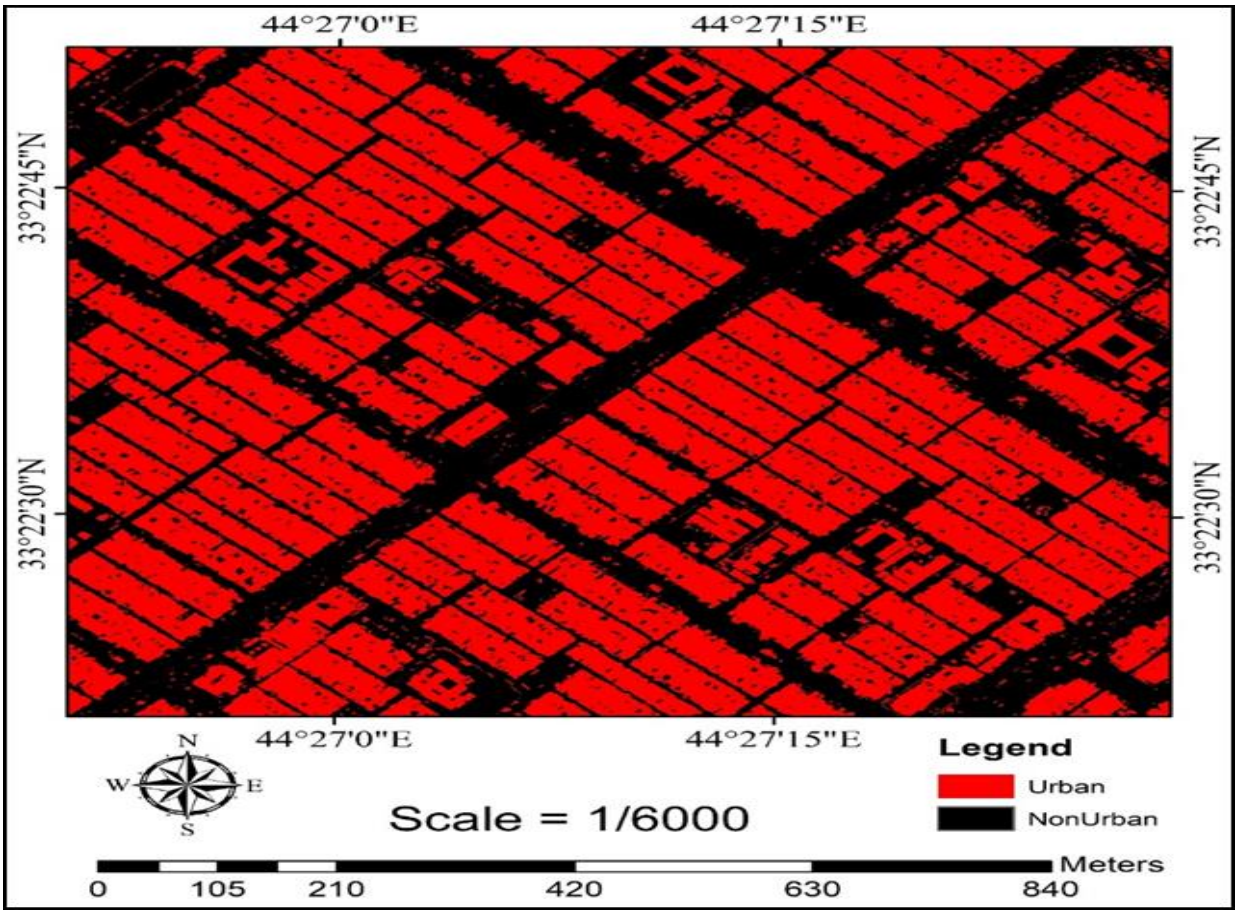

Fig. 5 shows the thematic map of Rusafa city produced by using the ANN model.

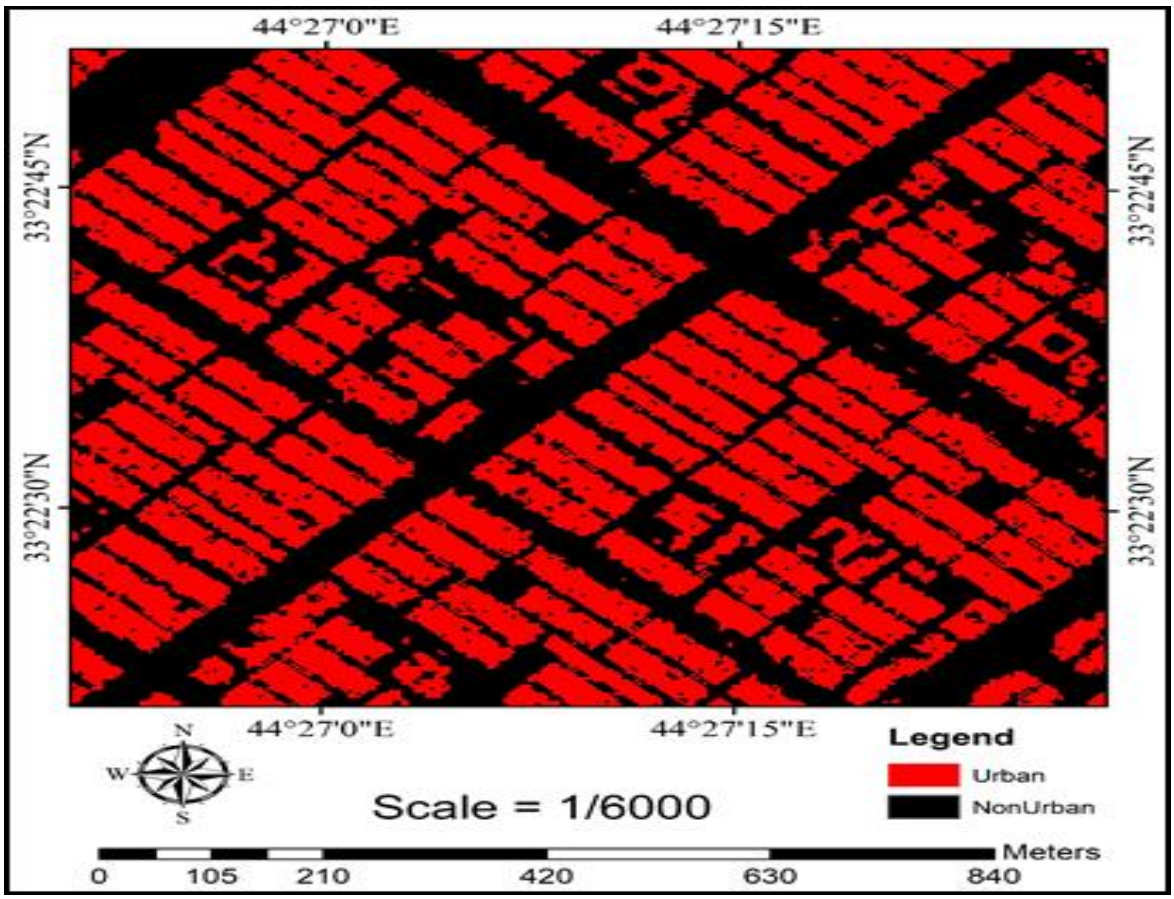

Fig. 6 shows the thematic map of Rusafa city produced by using the RF model.

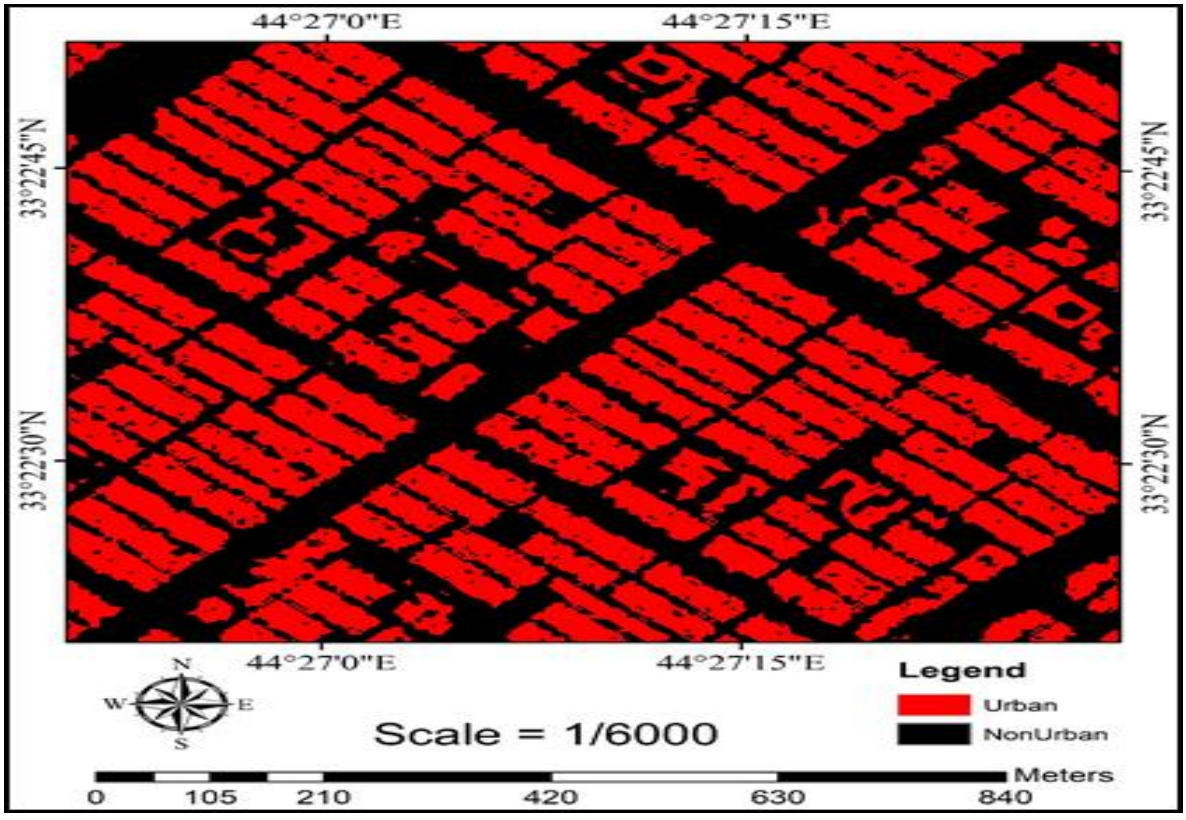

Fig. 7 shows the thematic map of Rusafa city produced by using the SVM model

5. CONCLUSION

Urban mapping has become increasingly important in recent time. As well as that, the extraction urban features from remotely sensed data and GIS are widely used in applications including forestry, agriculture, geology and landscape studies. In this work, different advance classification methods have been tested for the high-resolution satellite imagery classification for urban form Extraction. So the QuickBird image and the LiDAR data were used for the extraction urban area using object-based method. Then, both the image data and LiDAR-derived DSM were integrated based on the eCognition software and used for image segmentation by using the well-known multiresolution segmentation algorithm. Moreover, the samples have been urban and non-urban areas. In addition, the classifier used three algorithms such as Support Vector Machines (SVM), Random Forest (RF) and artificial neural network (ANN). The results were validated by two of indicators including Overall Accuracy and Kappa index. Finally, the results indicated that the ANN model performed the best compared to RF and SVM methods for thematic map of Rusafa city. ANN is a new computational model with rapid and large uses for handling various complex real world issues especially in image extraction. The ANN model achieved the highest training and testing accuracies of overall accuracy (98.80%) and Kappa index (0.96) and overall accuracy (96.32%) and Kappa index (0.94) for the training and testing samples, respectively.

REFERENCES

[1] Weng Q, Quattrochi D, Gamba P. Urban remote sensing. 2018.

[2] Sun Z, Xu R, Du W, Wang L, and Lu D. High-resolution urban land mapping in China from sentinel 1A/2 imagery based on Google Earth Engine. *Remote Sensing* 2019; **11**: 1-22 MdpiCom.doi:10.3390/rs11070752.

[3] Mohammed Albayati MA, Hashim Hamed N, Al any SJ. Detect irregularities of master plan by comparison with land use, using GIS and remote sensing techniques for Falujah city. *Iraqi Journal for Civil Engineering* 2017; **vol.2**.

[4] Jasim OZ, Hasoon KI, Sadiqe NE. Mapping LCLU Using Python Scripting. *Eng Technol J* 2019; **37**:140–7. https://doi.org/10.30684/etj.37.4A.5.

[5] Rizeei HM, Pradhan B. Urban Mapping Accuracy Enhancement in High-Rise Built-Up Areas Deployed by 3D-Orthorectification Correction from WorldView-3 and LiDAR Imageries. *Remote Sensing2019*. MdpiCom. https://doi.org/10.3390/rs11060692.

[6] Hashim Hameed N. On the use of GIS Technique to Analyze the Distribution of Primary Schools in Holy Karbala City. *Eng. &Tech. Journal* 2016: **Vol.34**: 2816-2827.

[7] Mohammed HR, Hamed NH, Al Bayati MM. Building of a Spatial Database to Identify Areas of Contamination by Mines and Hazardous Remnants of War by Using GIS (Analyti-cal Study / Basra Governorate). *Anbar Journal of Engineering Science*. 2018; **vol.7**.

[8] Zakariya Jasim O. Using of machines learning in extraction of urban roads from DEM of LIDAR data: Case study at Baghdad expressways, Iraq. *Periodicals of Engineering and Natural Sciences* .2019; **vol.7**:1710–21.

[9] Singh KK, Chen G, Ozelkan E, Zhou J, Brown MR, Meentemeyer RK. Uncertainties in mapping forest carbon in urban ecosystems. *Artic J Environ Manag* 2017. https://doi.org/10.1016/j.jenvman.2016.11.062.

[10] Näsi R, Honkavaara E, Blomqvist M.and Saarenmaa P. Remote sensing of bark beetle damage in urban forests at individual tree level using a novel hyperspectral camera from UAV and aircraft. *Elsevier*2018;**vol. 30**:72-83

[11] Abdelkarim A, Gaber AFD, Youssef AM, Pradhan B. Flood Hazard Assessment of the Urban Area of Tabuk City, Kingdom of Saudi Arabia by Integrating Spatial-Based Hydrologic and Hydrodynamic Modeling. *Sensors*2019; **19**. https://doi.org/10.3390/s19051024.

[12] Rizaludin Mahmud M, Hosaka T, Rizaludin Mahmud M, Numata S. Mapping an invasive goldenrod of Solidago altissima in urban landscape of Japan using multi-scale remote sensing and knowledge-based classification Satellite-based water yield mapping View project Spatial Hydroanalytics Research View project Original Articles Mapping an invasive goldenrod of Solidago altissima in urban landscape of Japan using multi-scale remote sensing and knowledge-

based classification. *Elsevier* 2019. https://doi.org/10.1016/j.ecolind.2019.105975.

[13] Atli Benediktsson J, Pesaresi M, Arnason K. Classification and Feature Extraction for Remote Sensing Images From Urban Areas Based on Morphological Transformations. IEEE Trans Geosci *Remote Sensing* 2003; **vol.41**. https://doi.org/10.1109/TGRS.2003.814625.

[14] Sensing HX-PE& R, 2007 undefined. 06-012.qxd. 2007.

[15] Myint SW, Gober P, Brazel A, Grossman-Clarke S, Weng Q. Per-pixel vs. object-based classification of urban land cover extraction using high spatial resolution imagery. *Elsevier* 2010. https://doi.org/10.1016/j.rse.2010.12.017.

[16] Abdulkareem A, Aldulaimi A, Pradhan B, Mansor S, Ahmed AA, Kalantar B, et al. Land Use and Land Cover Mapping Using Rule-Based Classification in Karbala City, Iraq deepgeo: Automated Classification of Remote Sensing Data with Deep Learning in Python View project LTA-UAV View project Land Use and Land Cover Mapping Using Rule-Based Classification in Karbala City, Iraq. *Springer* 2019; **vol.9**:1019–27. https://doi.org/10.1007/978-981-10-8016-6_71.

[17] Abdulkareem A, Aldulaimi A, Pradhan B, Al-Zuhairi M. An optimized object-based analysis for vegetation mapping using integration of Quickbird and Sentinel-1 data Flood Monitoring Mapping View project Application of fuzzy logic and GIS to provide geospatial solutions for displaced people in Al-Anbar province , *Iraq View project. Artic Arab J Geosci* 2018; **vol.11** https://doi.org/10.1007/s12517-018-3632-1.

[18] Chen Y, Fan R, Yang X, Wang J, Latif A. Extraction of Urban Water Bodies from High-Resolution Remote-SensingImageryUsingDeepLearning.*JournalWater*2018;**vol.10**.MdpiCom. https://doi.org/10.3390/w10050585.

[19] Priem F, Canters F, Yu B, Myint SW, Atzberger C, Thenkabail PS. Synergistic Use of LiDAR and APEX Hyperspectral Data for High-Resolution Urban Land Cover Mapping. *Remote Sensing*.2016; **vol.8** MdpiCom. https://doi.org/10.3390/rs8100787.

[20] Zhang W, Li W, Zhang C, Hanink DM, Li X, Wang W. Parcel-based urban land use classification in megacity using airborne LiDAR, high resolution orthoimagery, and Google Street View Remote sensing View project Markov chain geostatistical modeling View project Parcel-based urban land use classification in megacity using airborne LiDAR, high resolution orthoimagery, and Google Street View. *Elsevier* 2017; **vol. 64**. https://doi.org/10.1016/j.compenvurbsys.2017.03.001.

[21] Ibrahim Sameen M, Pradhan B. A Two-Stage Optimization Strategy for Fuzzy Object-Based Analysis Using Airborne LiDAR and High-Resolution Orthophotos for Urban Road Extraction. *Journal of Sensors*2017. HindawiCom.

[22] Li Q, Lu L, Jiang H, … JH-2018 FI,. Object-based urban land cover mapping using high-resolution airborne imagery and LiDAR data. *IeeexploreIeeeOrg n.d* 2018 undefined.

[23] Degerickx J, Roberts D,. Enhancing the performance of Multiple Endmember Spectral Mixture Analysis (MESMA) for urban land cover mapping using airborne lidar data and band. *Elsevier*2019 undefined.